





Engineering of Tracheal Grafts Based on Recellularization of Laser-Engraved Human Airway Cartilage Substrates

CARTILAGE
January-March 2022: 1–12
© The Author(s) 2022
DOI: 10.1177/19476035221075951
journals.sagepub.com/home/CAR


Denis Baranovskii^{1,2,3,4}, Jan Demner², Sylvia Nürnberger^{5,6}, Alexey Lyundup^{4,7}, Heinz Redl⁶, Morgane Hilpert², Sebastien Pigeot², Michael Krasheninnikov⁴, Olga Krasilnikova^{3,7}, Ilya Klabukov^{3,7} , Vladimir Parshin⁸, Ivan Martin² , Didier Lardinois¹, and Andrea Barbero² 

Abstract

Objective. Implantation of tissue-engineered tracheal grafts represents a visionary strategy for the reconstruction of tracheal wall defects after resections and may develop into a last chance for a number of patients with severe cicatricial stenosis. The use of a decellularized tracheal substrate would offer an ideally stiff graft, but the matrix density would challenge efficient remodeling into a living cartilage. In this study, we hypothesized that the pores of decellularized laser-perforated tracheal cartilage (LPTC) tissues can be colonized by adult nasal chondrocytes (NCs) to produce new cartilage tissue suitable for the repair of tracheal defects. **Design.** Human, native tracheal specimens, isolated from cadaveric donors, were exposed to decellularized and laser engraving–controlled superficial perforation (300 μm depth). Human or rabbit NCs were cultured on the LPTCs for 1 week. The resulting revitalized tissues were implanted ectopically in nude mice or orthotopically in tracheal wall defects in rabbits. Tissues were assayed histologically and by microtomography analyses before and after implantation. **Results.** NCs were able to efficiently colonize the pores of the LPTCs. The extent of colonization (i.e., percentage of viable cells spanning $>300 \mu\text{m}$ of tissue depth), cell morphology, and cartilage matrix deposition improved once the revitalized constructs were implanted ectopically in nude mice. LPTCs could be successfully grafted onto the tracheal wall of rabbits without any evidence of dislocation or tracheal stenosis, 8 weeks after implantation. Rabbit NCs, within the LPTCs, actively produced new cartilage matrix. **Conclusion.** Implantation of NC-revitalized LPTCs represents a feasible strategy for the repair of tracheal wall defects.

Keywords

regenerative medicine, tissue engineering, tracheal cartilage, laser perforation, nasal chondrocytes

Introduction

Airway defects arising congenitally or secondarily as a result of trauma, tracheal invasion by malignant tumors, or surgical resections are one of the most severe and life-threatening clinical conditions. Recent evidence suggests that patients with extended recurrent cicatricial stenosis are a leading value group among tracheal diseases. This frequency significantly increased in recent decades due to the capabilities of resuscitation, allowing treatment of extremely heavy patients with severe traumatic brain injury who required prolonged artificial lung ventilation via an endotracheal or tracheostomy tube. Primary reconstruction of extended tracheal defects is limited to 50% of the trachea in adults or 30% in children.¹

In light of recent events, it is becoming important to consider regenerative medicine as a novel approach for the

¹Thoracic Surgery, University Hospital Basel, Basel, Switzerland

²Department of Biomedicine, University Hospital Basel, University of Basel, Basel, Switzerland

³Department of Regenerative Technologies and Biofabrication, National Medical Research Radiological Center, Obninsk, Russia

⁴Research and Educational Resource Center for Cellular Technologies, Peoples' Friendship University of Russia, Moscow, Russia

⁵Division of Trauma Surgery, Department of Orthopedics and Trauma Surgery, Medical University of Vienna, Vienna, Austria

⁶Ludwig Boltzmann Institute for Experimental and Clinical Traumatology, AUYA Research Center, Vienna, Austria

⁷Department of Advanced Cell Technologies, Sechenov University, Moscow, Russia

⁸Institute of Clinical Medicine, Sechenov University, Moscow, Russia

Corresponding Author:

Ivan Martin, Department of Biomedicine, Tissue Engineering Laboratory, University Hospital Basel, University of Basel, Basel, 4031, Switzerland.
Email: ivan.martin@usb.ch



treatment of airway defects. Tracheal tissue engineering has been an object of research since the 1990s. Several approaches for tracheal tissue engineering, including the use of autologous or allogeneic cells, and scaffolds derived from different synthetic materials or natural tissues have been reported.² However, despite the proliferation of studies and reported attempts at tracheal reconstruction in patients,³ there is still no consolidated approach that would provide suitable, engineered trachea grafts. The described techniques have had limited success, possibly due to the lack of living cells in cartilage structures, leading to the lack of new cartilage matrix production and finally to aseptic necrosis and progressing malacia.⁴ At the same time, the “ideal” prototype of a tissue-engineered tracheal graft should not only contain a sufficient amount of viable regenerative cells but also have physiologically relevant mechanical properties⁵ to promote stable, tracheal lumen repair at the implantation site.

Native tracheal cartilage (TC) has already gained attention as a promising material for the creation of biocompatible scaffolds to be seeded with chondrocytes to generate functional grafts.^{6,7} However, the highly dense matrix of the airway cartilage may limit cells from deep tissue colonization.

Several approaches including perforation, ultrasonic cavitation, and detergent-enzymatic treatment have been proposed to enhance the viability and the migration of the cells used for the revitalization of the constructs.⁸⁻¹¹ Introduction of channels in the scaffold is an effective method resulting in increased cell colonization.¹² One of the main concerns is that a high porosity would reduce the stiffness of the scaffold. In this study, we used a technique that allows the attainment of high perforation density of the decellularized tracheal scaffold by laser engraving saving scaffold stiffness enough to provide stability of the tracheal lumen during inhalation.

Another important aspect to be considered to revitalize the scaffold is the utilization of the proper cell type to use for the revitalization of the scaffold—cells that must possess a good capacity to engraft in a diseased environment and be capable of producing a high-quality cartilage matrix. In this regard, human nasal chondrocytes (hNCs) have been shown to exhibit a higher proliferation capacity and a higher and more reproducible chondrogenic capacity after *in vitro* expansion when compared with other chondrocytes.^{13,14} hNCs were recently demonstrated to be able to respond and adapt to heterotopic transplantation sites¹⁵ and to possess superior ability over mesenchymal stromal cells (and articular chondrocytes) to survive/perform even when exposed to inflammatory/degenerative conditions.¹⁶ Finally, cartilage grafts engineered with hNCs were clinically used to reconstitute the nasal alar lobule¹⁷ and to repair articular cartilage defects.¹⁸

This study is aimed at investigating the capability of NCs to colonize the pores of decellularized laser-perforated tracheal cartilage (LPTC) tissues and to newly produce a cartilage matrix. In addition, we performed a proof-of-principle study in rabbit to test the feasibility of using NC-revitalized LPTCs for the repair of TC defects.

Materials and Methods

Harvest and Decellularization of Human TC

TC tissues were harvested from human cadavers that met the following criteria: ≥ 18 years old at the moment of death, and no trachea-bronchial diseases, infections, disorders, or malignancies. All procedures were conducted with the approval of the Local Ethics Committee of Sechenov University (July 15, 2015, protocol N. 07-15). The trachea samples were isolated between the second tracheal ring and the carina. The tracheal rings were carefully separated from all surrounding tissues using a surgical blade. Separated tracheal rings were sliced into small samples (2×5 mm). TC samples were decellularized using the freeze and thaw method.¹⁹ In brief, the samples were placed into cryovials that were immersed into liquid nitrogen for 15 minutes, and samples were then thawed in a water bath at 37°C for 30 minutes. This cycle was repeated 5 times. Decellularized samples were assayed using the toxicity controls described below. Samples that passed these controls were packed in an ice-cold phosphate-buffered saline (PBS) containing 100 U/ml penicillin and 100 mg/ml streptomycin, and labeled and delivered to the Tissue Engineering Lab (University Hospital of Basel, Switzerland) or the Division of Trauma-Surgery of the Medical University of Vienna in a plastic box, equipped with cold packs and thermologger device. All shipment in our study were deposited in specially labeled plastic boxes abiding with procedures and regulations in accordance with the Russian, Swiss, and European Union (EU) requirements.

Laser Perforation (Engraving) of Decellularized Tracheal Cartilage (dTTC)

Perforation of dTTC was performed with a laser engraver “Trotec Speedy 300” (Trotec Ltd, Austria) with a standard wavelength of $10.6\ \mu\text{m}$ and a pulse duration of 0.2 ms. The laser was set at 30 W and operated with a speed of 42.6 cm/s. To engrave the grooves, circles of $10\ \mu\text{m}$ were drawn at a 250- μm distance. LPTCs were divided into smaller pieces (2×2 mm) and assessed with scanning electron microscopy (SEM) and histologically (as described below), or used for the revitalization studies before being exposed to the following sterilization process. LPTCs were incubated for 1 hour with 70% ethanol (under agitation), and samples were then rinsed 4 times with sterile PBS (1 day per wash,

with change of PBS each day) under agitation. Samples were subsequently assessed with the quality controls described below.

Safety and Quality Control of dTCs and LPTCs

Samples (dTCs and LPTCs) were placed in sterile 15 ml Eppendorf (4 samples/tube) and incubated for 3 days at 37 °C and 5% CO₂ with Dulbecco's Modified Medium (DMEM; Gibco, USA) (2ml/tube). Tubes containing only DMEM (controls, ctr) were incubated in the same conditions. Conditioned medium from dTCs (dTC-CM), conditioned medium from LPTCs (LPTC-CM), and control medium (ctr-M) were then harvested and used for endotoxin and cytotoxicity tests. It was decided to consider non-toxic the samples that fulfilled both these criteria (currently in use in our phase II clinical trial, [clinicaltrials.gov: NCT02673905](https://clinicaltrials.gov/ct2/show/study/NCT02673905)): more than 90% cell viability in cytotoxicity test, less than 1.0 IE/ml of endotoxin.

Endotoxin quantification. The concentration of endotoxins in the collected media (ctr-M, dTC-CM, and LPTC-CM) was measured at the Hospital Pharmacy Basel using the Limulus Amebocyte Lysate assay (chromogenic kinetic method), a lysate that reacts with bacterial endotoxin lipopolysaccharide, which is a membrane component of gram-negative bacteria.

Cytotoxicity test. Passaged 2 hNCs were placed in 24-well plates (10,000 cells/well) and cultured in Expansion medium (EM, see below) up to the confluency. Resulting cell layers were then rinsed with PBS and exposed to the following media: dTC-CM:EM (1:1), LPTC-CM:EM (1:1), and ctr-M:EM (1:1) for 48 hours. hNCs were then detached with 0.05% Trypsin-EDTA (Gibco) and counted with Trypan blue (Sigma-Aldrich) to measure cell number and viability.

Isolation and Culture of NCs

Human nasal chondrocytes. Nasal septum biopsies were received from patients ($n = 5$, 4 women and 1 men, 25-54 years old; mean age, 35.6 years) undergoing rhinoplasty after informed consent and in accordance with the local ethical commission (EKNZs; Ref.# 78/07). Remnants of perichondrial tissues, when present, were carefully removed from the biopsies by a trained personnel to avoid having contaminant perichondrial cells in the culture.²⁰ Pure nasal cartilage biopsies were then digested for 22 hours with 1.5 mg/ml collagenase type II (BioConcept).²⁰ The isolated hNCs were expanded in EM (DMEM containing 10% fetal bovine serum [FBS], 10 mM HEPES buffer [Gibco], 1 mM sodium pyruvate [Gibco], 100 U/ml penicillin, 100 µg/ml streptomycin, 0.29 mg/ml L-glutamine [Invitrogen], 1 ng/ml TGF-β1 and 5 ng/ml FGF-2 [both from R&D Systems])

for 2 passages. Passaged 2 hNCs were then used for the revitalization of LPTCs as follows.

Rabbit nasal chondrocytes (rNCs). rNCs were harvested according to Chen et al.²¹ Allogeneic rNCs were isolated from the nasal septum biopsy of 2 adult male rabbits (3.2-3.5 kg) under total anesthesia. Briefly, the cartilage specimens were cut into small slices and digested at 37 °C with 0.15% protease from *Streptomyces griseus* (Sigma-Aldrich) in Hank's balanced sodium salt (Invitrogen) for 30 minutes. Slices were then digested overnight at 37 °C with 0.025% type II collagenase (BioConcept) in DMEM (Invitrogen, Carlsbad, CA) on a magnetic stirrer. Finally, the isolated rNCs were cultured in EM (not containing TGF-β1) for 2 passages.

Revitalization of LPTCs

LPTCs were placed onto 0.4 mm pore-size polycarbonate Transwell filters (Corning B.V. Life Sciences, Schiphol-Rijk, The Netherlands; 2 samples/insert). hNCs or rNCs were loaded on the top of the LPTCs (100 µl of cell suspension containing 0.5×10^6 cells per insert) in Chondrogenic Medium, high-glucose DMEM containing 5% FBS, 10 mM HEPES, 1 mM sodium pyruvate, 100 U/ml penicillin, 100 µg/ml streptomycin, 0.29 mg/ml L-glutamine, 10 µg/ml insulin (Novo Nordisk, Bagsvaerd, Denmark), and 0.1 mM ascorbic acid 2-phosphate (Sigma-Aldrich) for 7 days at 37 °C and 5% CO₂ with media changes twice/week. Revitalized LPTC constructs with hNCs were assessed histologically and biochemically as described below or implanted subcutaneously in nude mice (see below description). Revitalized LPTC constructs with rNCs were implanted orthotopically in rabbit (see below description).

In Vivo Experiments

Ectopic study in nude mice. We investigated the capacity of hNCs to further migrate into the *in vitro* revitalized LPTCs and to produce a new cartilaginous matrix implanting the tissue in nude mice. All animal procedures were reviewed and approved by the Swiss Federal Veterinary Office (permission # 1797). Briefly, hNC-revitalized LPTCs ($N = 4$) and non-revitalized LPTCs ($N = 2$, control) were implanted in the subcutaneous pockets of CD1 nu/nu female nude mice (4-6 weeks old, $n = 2$) (4 samples/mouse). The operation was performed with isoflurane (Attane Isoflurane; Provet AG, Lyssach, Switzerland) anesthesia and buprenorphine (Temgesic; Reckitt Benckiser AG, Wallisellen, Switzerland) analgesia, and animals were checked periodically. After 28 days, mice were euthanized with CO₂ and explants were assessed as described below.

Orthotopic study in rabbits. We investigated the capability of *in vitro* revitalized LPTCs to heal tracheal lesions in an

orthotopic rabbit model. The Local Ethics Committee of the Sechenov University approved experimental studies on animals (protocol No 07-15 July 15, 2015). rNC-revitalized LPTCs and non-revitalized LPTCs (control) were implanted in experimentally induced defects in the tracheal wall of rabbits (female Gray Giant Flander rabbits, 3-6 months of age). Animals were operated under general anesthesia with Zoletil 100 (Virbac, France). The anterior and anterolateral tracheal wall of the neck tracheal region was visualized and mobilized. A tracheal wall defect approximately 6×4 mm was formed by the resection of the anterior tracheal wall within 4 tracheal rings below the second ring. Rabbits were randomly divided into 2 groups according to the constructs to be implanted: (1) control ($N = 4$) and (2) revitalized ($N = 4$). LPTCs were grafted in the tracheal defects in a way that the smooth unperforated side conforms with the inner tracheal surfaces and were fixed with separate sutures (Prolene 7-0). The rabbits were monitored weekly for their activity and vital parameters including their heart rate, breathing rate, and oxygen saturation.

Multislice computed tomography was performed for 2 rabbits (one for control and one for the revitalized group) 4 weeks after surgery. All rabbits were euthanized by CO_2 asphyxiation 8 weeks after surgery. The whole trachea from the first tracheal ring to carina was explanted for the radiological and histological analysis.

Analytical Methods

Scanning electron microscopy. The samples were fixed overnight in 0.05% glutaraldehyde at 4 °C, dehydrated in graded ethanol concentrations, and processed via “critical point drying” (CPD). SEM (Nova NanoSEM 230, FEI, USA, Acc: 5000 Volt, Detektor: 8000, Iteration: 22700 nA) of LPTCs was performed after a gold sputter-coating in vacuum. A piece of native human dTC was used as a control sample.

Quantification of DNA. Five dTCs derived from a TC sample were assessed to quantify the contents of DNA. Samples were washed in PBS and digested with protease K (0.5 ml of 1 mg/ml protease K in 50 mM Tris with 1 mM EDTA, 1 mM iodoacetamide, and 10 mg/ml pepstatin-A for 15 h at 56 °C). DNA amounts were spectrofluorometrically measured using the CyQUANT Kit (Molecular Probes, Eugene, OR) and with calf thymus DNA as a standard.¹⁶ Results were normalized by the weight of the samples.

Histology. All samples were fixed in 4% paraformaldehyde for 24 hours at room temperature and dehydrated in a graded ethanol series, embedded in paraffin, and cut into 5- μm -thick serial sections with the microtome (Thermo Fisher Scientific, USA) inserting 5 trimming steps of 25 μm to obtain the slides from superficial and deep zones separately. Slices were then incubated at 56 °C for 30 minutes, and dewaxed and stained with Safranin-O (Saf-O) according to

standard protocols. Histological images were acquired with a microscope (Eclipse Ti2; Nikon Corp., Tokyo, Japan). Saf-O-stained slides from *in vitro* and *in vivo* (nude mice) samples were scored using the established Bern Score, according to Grogan et al.,²² to assess the quality of the newly formed cartilage tissues within the pores of the LPTCs or used to quantify the number of cells within the pores as described below. Bern Score grading and estimation of cell numbers were performed on slides derived from superficial (0-100 μm) or deep (200-400 μm) zones. For each zone, a total of 30 to 50 pores corresponding to a total area of 500 μm^2 were examined. Saf-O-stained slides ($N = 5/\text{group}$, corresponding to a total area of 0.15 cm^2) from *in vivo* (rabbit) samples were scored to quantify the percentage of glycosaminoglycans (GAG)-positive areas.

Quantitative real-time reverse transcriptase polymerase chain reaction (qRT-PCR). Total RNA was extracted from expanded hNCs and from *vitalized* LPTCs. cDNA synthesis and qRT-PCR (7300; Applied Biosystems) were performed as previously described²⁰ to quantify the expression levels of type I collagen (Col I, Hs00164004), type II collagen (Col II, Hs00264051), aggrecan (Agg, Hs00153936 m1), and versican (Ver, Hs00171642 m1) (all from Applied Biosystems). For each sample, the Ct value of each target sequence was subtracted from the Ct value of the reference gene (human GAPDH, Hs02758991k Applied Biosystems) to derive the ΔCt .

ALU in situ hybridization. ALU *in situ* hybridization was performed on samples explanted from the nude mice to access the human origin of the cells, according to a standard protocol. The *in vivo* samples were deparaffinized and digested with Pepsin (Sigma, USA), 0.5 mg/ml 0.01 N HCl for 10 minutes at 37°C, and then neutralized by acetic anhydride. Prehybridization was done with bovine DNA (5 mg/ml) in 50% dextran sulfate and SSC buffer. Hybridization was done with the ALU-probe (Microsynth, Switzerland) for around 16 hours, at 42 °C. For detection, a pretreatment with α -DIG conjugated to alkaline phosphatase (anti-digoxygenin-AP; Roche, Switzerland) was used with an incubation in NBT/BCIP substrate (Roche, Switzerland) in DIG-3 buffer and counterstain with Nuclear Fast Red for 1 minute (Sigma, USA).

Immunohistochemistry. Immunostaining was performed following the standard protocol for paraffin-embedded samples²³ using EnVision (DAKO Cytomation) or Vectastain ABC detection kit (Linaris). Briefly, the samples were deparaffinized with xylol and ethanol, enzymatically digested with 0.2% hyaluronidase (3,000 U/mg; Sigma-Aldrich) and 0.1% pronase (Sigma-Aldrich) for 30 minutes each, treated with goat serum (Invitrogen), and finally stained against pan-cytokeratin (CK-Pan monoclonal mouse antibody diluted 1:100; Sigma-Aldrich) using

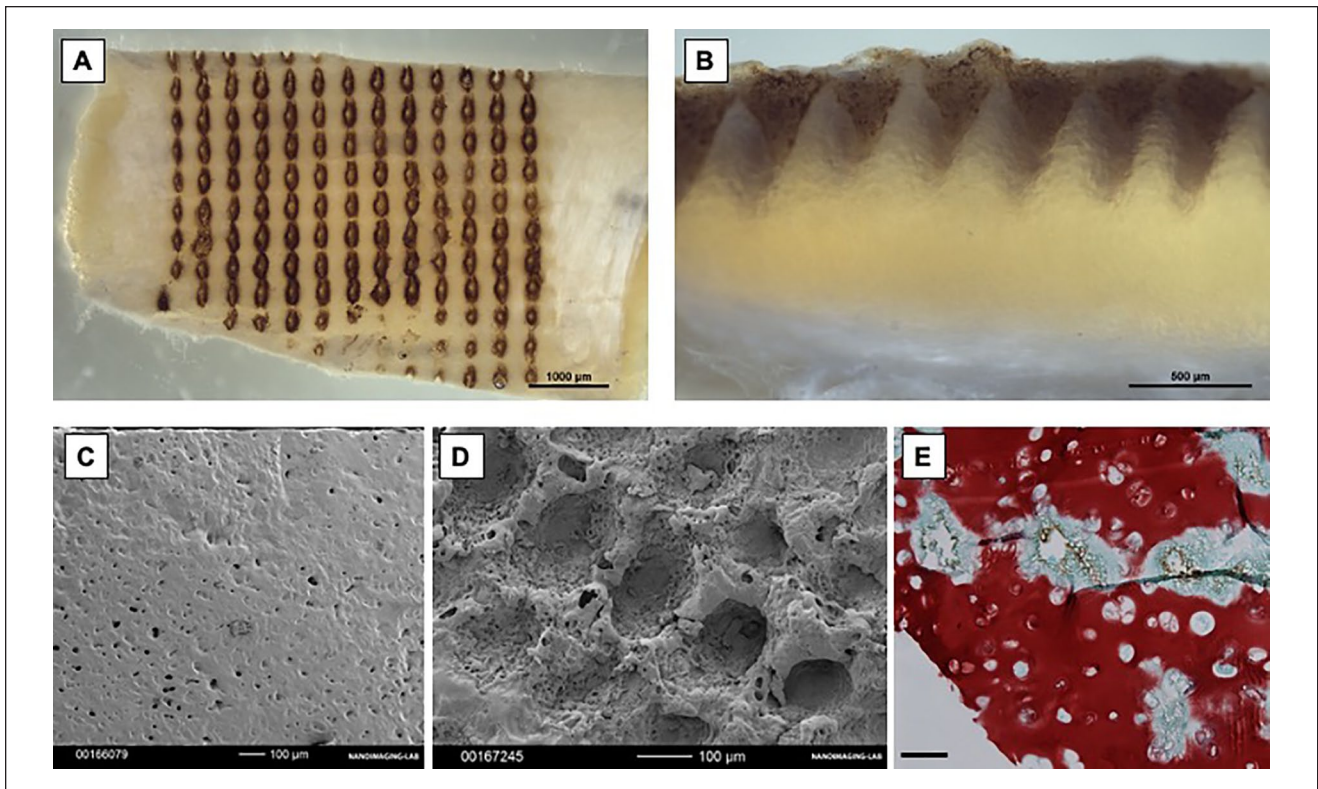


Figure 1. Performance of the laser perforation on decellularized tracheal cartilage (dTC) tissues. (A, B) Macroscopic appearance of laser-perforated tracheal cartilage (LPTCs). (C, D) Representative SEM pictures. (E) Safranin-O staining of representative LPTCs. NC = nasal chondrocytes; SEM = scanning electron microscopy.

secondary goat anti-mouse antibodies (Sigma-Aldrich). Vector Red AP Substrate kit with Levamisole (Linaris) was finally applied for brown or red staining.

Microtomography (μ CT). Micro-CT with Skyscan 1276 (Bruker, USA) was performed for LPTC samples embedded in paraffin at 15 kV, 15 mA, 2,500 ms exposure, and rotation angle of 0.5° at a resolution of 20 μ m.

Statistical Analyses

Statistical evaluation was performed using SPSS software version 22 (SPSS, Sigma Stat). Data were represented as mean \pm SD (standard deviation). Differences between groups were estimated by Kruskal-Wallis followed by Mann-Whitney tests and *P* values adjusted with Bonferroni correction. Comparisons of 2 groups were performed by a Mann-Whitney test. *P* values <0.05 were considered statistically significant.

Results

Characterization of LPTCs

Gross appearance images showed a regular distribution of pores (9 pores/ mm^2) in the LPTCs (Fig. 1A and B), which by SEM analysis appeared to have a regular size (ca 200 μ m

diameter and 300 μ m depth) (Fig. 1C and D). Safranin-O staining evidenced a certain loss of GAG only in the regions immediately surrounding the pores but a preserved GAG intense matrix in the remaining regions of the LPTCs (Fig. 1E). Overall, these results indicate that laser perforation induced a regular porosity on the dTCs without causing major alterations of the cartilaginous matrix of the TC tissues.

Safety and Quality Controls

DNA content of TCs after the decellularization process averaged 35 ± 12 ng/mg, that is, similar to amounts reported in previous studies.^{24,25} To test the safety of the TC tissues, conditioned media were generated from dTCs and LPTCs and assessed for their cytotoxicity or assayed to quantify the concentration of endotoxins. Results showed that endotoxin concentrations were similarly low (less than 1.0 IE/ml) in the conditioned media and control medium (Table 1). Results from the cytotoxic study demonstrated a comparable number of cells and cell viability of hNCs exposed for 48 hours to the conditioned media or the control medium (Table 1). These results indicate the safety of the processed TC samples that were thus used for the revitalization studies.

Table I. Safety and Quality Control Tests.

		Control Medium	CM from dTCs	CM from LPTCs
I	Endotoxin conc. (IE/ml)	0.54 ± 0.05	0.61 ± 0.09	0.65 ± 0.07
II	No. of cells counted ($\times 10^5$)	1.9 ± 0.2	1.6 ± 0.4	1.7 ± 0.1
III	Viability (%)	99.0 ± 1.2	98.8 ± 2.5	97.5 ± 3.1

dTC = decellularized tracheal cartilage; hNC = human nasal chondrocytes; LPTC = laser-perforated tracheal cartilage.

I: Endotoxin concentration measured in control medium or in conditioned media (CM) generated from dTCs or LPTCs. Number of human nasal chondrocytes (hNCs) (II) and percentage of viable hNCs (III) after 48 hours of exposure to the different media. Values are mean ± SD of 3 independent experiments.

Revitalization of LPTCs With hNCs and Ectopic In Vivo Study

hNCs were cultured on the surface of the LPTCs for 7 days to assess their capacity to repopulate *in vitro* the pores of the TC grafts. Histological analyses of *in vitro* revitalized samples showed that the majority of the pores (>90%) were colonized by hNCs. The hNCs within the pores had a fibroblastic morphology and were surrounded by a loose GAG-negative matrix (Fig. 2A). qRT-PCR analyses demonstrated that hNCs cultured in the LPTCs versus post-expanded hNCs expressed higher levels of the chondrogenic genes Agg (12.3-fold, $P < 0.05$) and Col II (23.5-fold, $P < 0.05$) and lower levels of the fibrocartilaginous genes Ver (7.6-fold, $P < 0.05$) and Col I (3.0-fold, $P = 0.06$) (Fig. 2B), thus indicating the onset of redifferentiation of the hNCs in the pores of the LPTCs. Revitalized and non-revitalized (ctr) LPTCs were also implanted ectopically in nude mice to assess the extent of colonization and further matrix deposition by hNCs in an *in vivo* environment. The pores of the revitalized LPTCs explanted from the mice were filled with newly formed tissues consisting of cells with a mixed fibroblastic and round morphology and a dense extracellular matrix variably stained for GAG (Fig. 2C and D). A ring of dense matrix lining the edges of the holes and confining the hNCs can be observed (see brown ring in the images of Fig. 2). However, in a few pores (ca 10%), this ring was partially digested; thus, the hNCs could exit from the hole, colonize the neighboring extracellular matrix (ECM), and produce a new GAG-positive matrix (Fig. 2D). In non-revitalized LPTCs, pores remained void (>30%) or were partially filled with fibroblastic/inflammatory cells (Fig. 2D). Saf-O-stained sections from the *in vitro* and *in vivo* revitalized LPTCs were further assessed to quantify cellularity (i.e., number of cells/pore) and to grade the quality of newly formed tissue (using the Bern Score grading system) at different depths (superficial: 0–100 μm vs deep: 200–400 μm). We observed that the pores of both *in vitro* and *in vivo* revitalized LPTCs contained similar amounts of cells at different depths (Fig. 3A), thus indicating a uniform colonization of the pores. Tissues filling the pores of the *in vivo* samples had higher scores compared with the *in vitro* ones. No statistically

significant differences in the scores of tissues from superficial and deep areas were observed (Fig. 3B).

ALU staining of the *in vivo* samples (Fig. 4) demonstrated the human origin of the cells within the pores of the revitalized LPTCs. Limited/nil amounts of ALU-positive cells were detected in the LPTC matrix surrounding the pores, indicating limited migration of the cells from the holes into the cartilage.

Overall, these results indicate the capacity of hNCs to efficiently colonize the LPTCs and to newly produce cartilaginous matrix within the pores.

Revitalization of LPTCs with rNCs and Orthotopic In Vivo Study

LPTCs were revitalized with precultured allogenic rNCs for 7 days *in vitro* and implanted in tracheal wall defects in rabbits. Animals in the control group received non-revitalized LPTCs.

LPTC grafts could be successfully fixed in the tracheal wall defects of all rabbits (Fig. 5A). All the rabbits were euthanized 8 weeks after the implantation without any signs of respiratory distress or infection during the period of observation. A CT scan 4 weeks after the orthotopic implantations revealed normally sustained tracheal structures with stable lumens and no evidence of graft deformation or tracheal stenosis in all of the recipients (Fig. 5B and C). Further micro-CT analysis and histological analyses of explanted samples, 8 weeks after surgery, demonstrated the stable position of the grafts closing tracheal defects (Fig. 5D and E).

Furthermore, Saf-O staining demonstrated that explanted tissue from rabbits operated with revitalized LPTCs contained a more abundant GAG-positive matrix when compared with those operated with non-revitalized LPTCs and that lacunae were partially filled with cells or remained void, respectively, in the revitalized or non-revitalized samples (Fig. 5FI–IV). Quantification of Saf-O images revealed a significantly higher percentage of GAG-positive area in the revitalized versus non-revitalized LPTCs ($15.1\% \pm 3.2\%$ vs $1.2\% \pm 0.5\%$, $P < 0.05$). Considering that the GAG-positive matrix was mainly pericellular and present only in the revitalized group, it is reasonable that the GAG

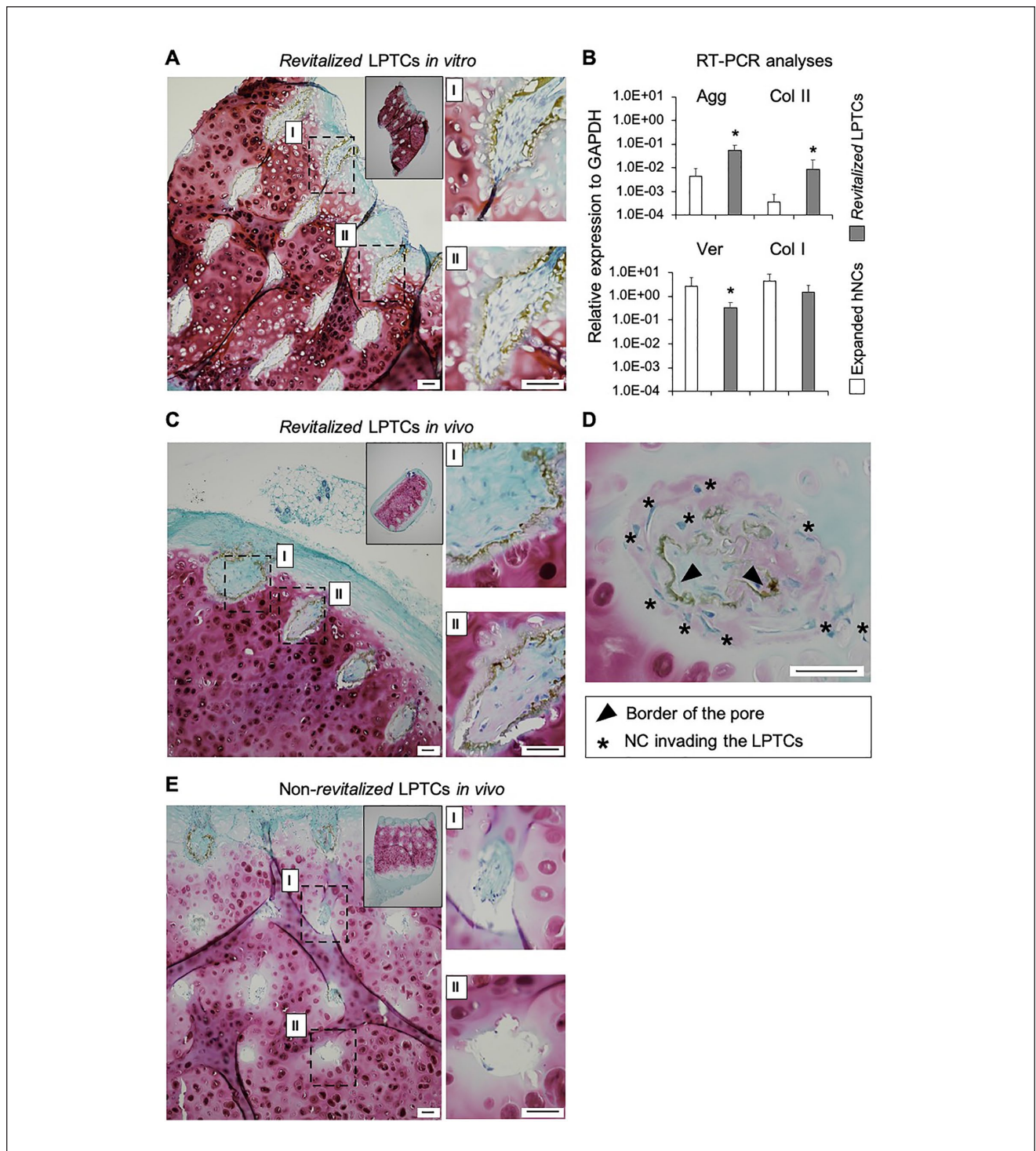


Figure 2. Capacity of human nasal chondrocytes (hNCs) to revitalize LPTCs *in vitro* and *in vivo* (ectopic study). Safranin-O staining of representative *in vitro* revitalized LPTCs (**A**). Real-time reverse transcriptase polymerase chain reaction analysis of post-expanded hNCs and *revitalized* LPTCs; values are mean \pm standard deviation of samples from 5 different donors. * $P < 0.05$ versus the corresponding expanded hNCs group (**B**). Safranin-O staining of representative revitalized LPTCs (**C**, **D**) and non-revitalized (ctr) LPTCs (**E**) explanted from the mice. Insets are low magnification images of the entire constructs. Images (I) and (II) are high magnification pictures of the corresponding dashed rectangular areas in (**A**), (**C**), and (**E**). The high magnification image in (**D**) shows some hNCs exiting the pore and colonizing the neighboring ECM. Scale bars = 100 μ m. ECM = extracellular matrix; LPTC = laser-perforated tracheal cartilage; NCs = nasal chondrocytes.

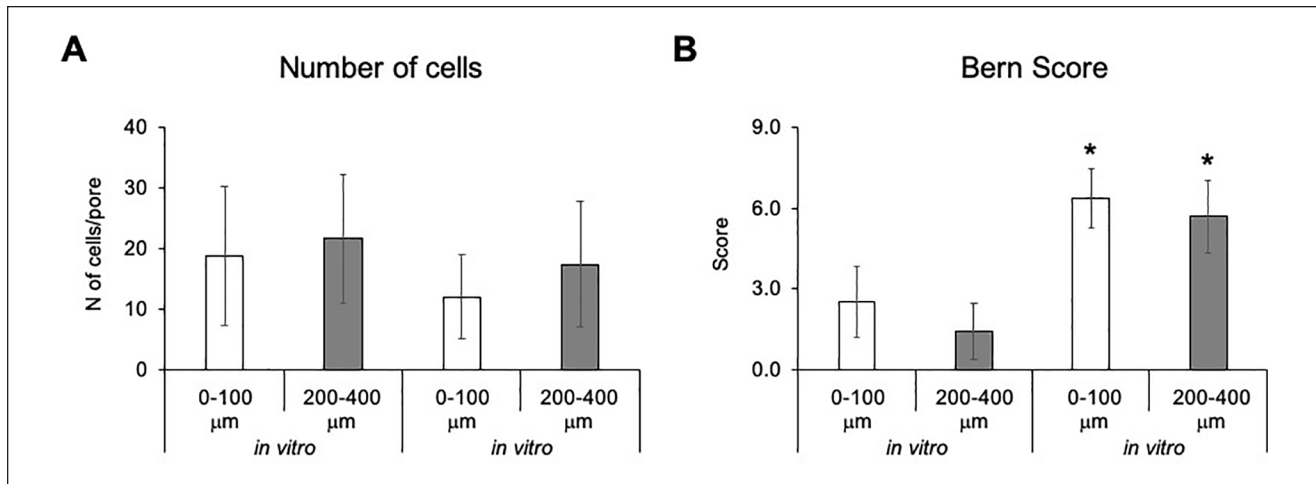


Figure 3. Number of cells/pores (A) and Bern Score grading (B) estimated in superficial (0-100 μm) and deep (200-400 μm) areas of the laser-perforated tracheal cartilage (LPTCs). Values are mean ± standard deviations of measurements performed on a total of 30-50 pores. Asterisks (*) indicate statistically significant differences ($P < 0.05$) from the corresponding *in vitro* samples.

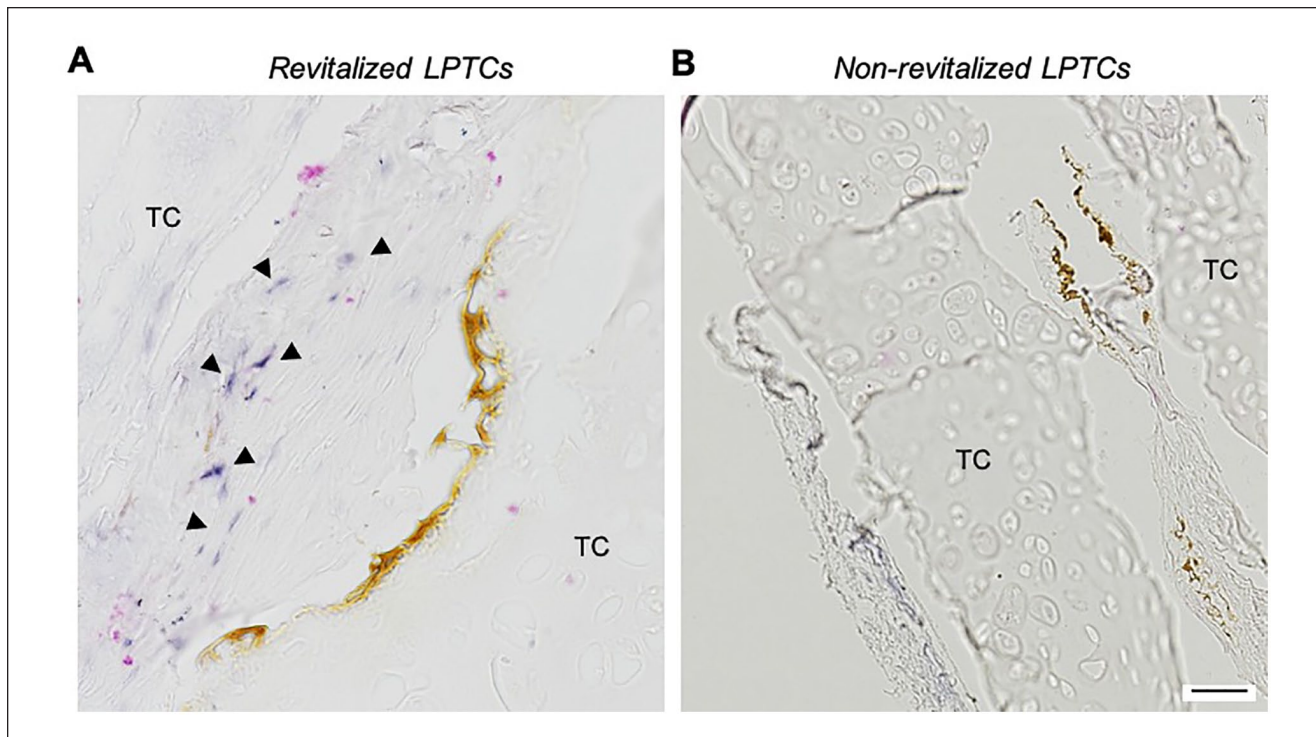


Figure 4. Origin of the cells in the LPTCs, *in vivo* ectopic study. ALU staining of representative revitalized (A) and non-revitalized (control) (B) LPTCs. Triangles show ALU-positive cells (i.e., cells of human origin). Scale bar = 100 μm. LPTC = laser-perforated tracheal cartilage; TC = native tracheal cartilage.

was newly produced by the transplanted nasal chondrocytes. Immunohistochemical analyses showed that both the revitalized and non-revitalized groups were fully covered by newly formed, pan-cytokeratin-positive respiratory mucosa (Fig. 5FV-VI).

Discussion

In this study, we demonstrated that NCs, that is, cells already used in clinics for the repair of cartilage defects,^{17,18} efficiently colonize the pores of the LPTCs and produce

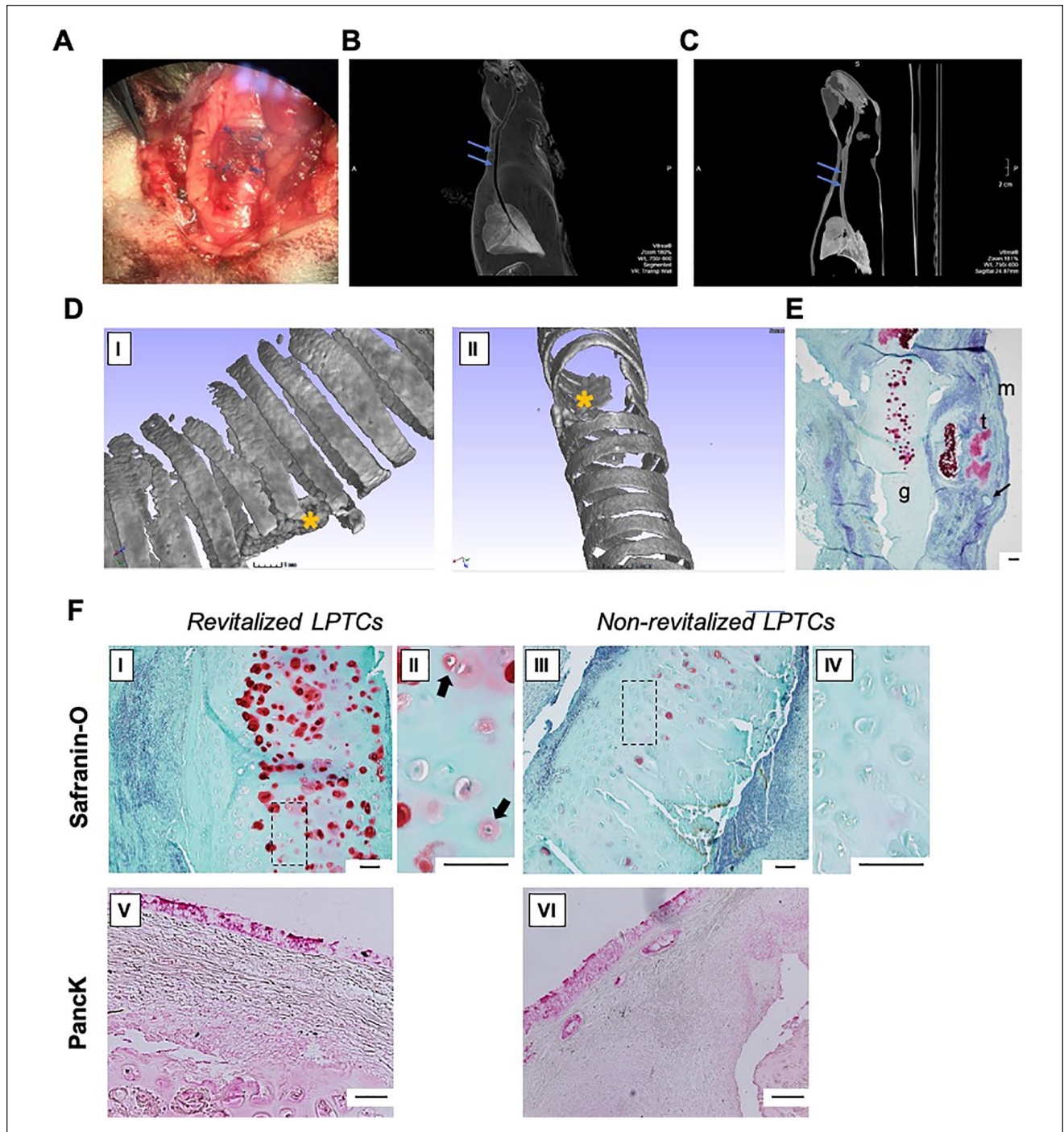


Figure 5. *In vivo* orthotopic study. (A) LPTC graft fixed in rabbit tracheal wall defect, macro image; (B, C) Rabbit chest and neck CT scan, 4 weeks after the orthotopic implantation of revitalized (B) and non-revitalized (C) LPTC; blue arrows indicate the position of the grafts; (D) micro-CT with 3-dimensional reconstruction of explanted tracheal samples harvested from rabbit operated with revitalized (I) and non-revitalized (II) LPTC; yellow asterisks indicate the position of the grafts. (E) Safranin-O pictures of the explanted tracheal sample harvested from rabbit operated with revitalized LPTC; g: LPTC graft, t: native rabbit tracheal lumen, m: mucosa in the tracheal lumen, arrow: PROLENE suture. (F) Representative histological (Safranin-O) (I–IV) and immunohistochemical (pan-cytokeratin, PancK) (V and VI) staining of tracheal samples harvested from rabbit operated with revitalized and non-revitalized LPTCs. II and IV are high magnification images of I and II, respectively. Black arrows indicate viable cells (i.e., nasal chondrocytes) within lacunae and surrounded by newly produced GAG-positive matrix. Scale bars = 100 μ m. CT = computerized tomography; GAG = glycosaminoglycans; LPTC = laser-perforated tracheal cartilage.

cartilaginous matrix *in vivo*. This study additionally provided evidence that the LPTCs revitalized with rabbit NCs supported stable reconstruction of TC defects and *de novo* formation of cartilaginous structures.

Decellularized cartilage matrices (that can be used in an allogenic setting) are considered viable scaffolds for the repair of TC defects.² However, these biological materials, made of a highly dense extracellular matrix, must be properly prepared to increase their porosity and thus allow for an efficient colonization by cells (*in vitro* and/or *in vivo*).

Recent studies have shown that laser perforation is an effective method to tune the porosity of cartilage tissues and, at the same time, preserve their original mechanical properties and the supporting *de novo* synthesis of cartilage matrix ectopically in nude mice^{24,26} or orthotopically in the joints of rabbits.²³ To our knowledge, the study by Xu et al.²⁵ was the only one in which TC was exposed to laser perforation. However, in their study, rabbit trachea (i.e., tissue much thinner than human trachea), lasered to generate superficial pores (200 μm in depth), was revitalized with rabbit auricular chondrocytes. In our study, a more clinically relevant approach was used, that is, human TC, laser perforated to generate deeper pores (300 μm), was revitalized with hNCs.

Our study did not investigate the mechanical properties of the LPTC samples. The previously mentioned study of Nürnbergger et al.²⁴ showed that laser-engraved articular cartilage (i.e., CartiScaff) retained more than half of its native compressive modulus, leaving the CartiScaff still more than 14 times stronger than commercially available scaffolds. This provided a relevant rationale that our LPTC would be mechanically compatible for implantation in tracheal wall defects.

Detailed examination of the *in vitro* cultured revitalized LPTC samples demonstrated uniform distribution of hNCs within the pores. However, due to the short culture time considered in this study, a limited cartilage matrix was deposited by the hNCs into the pores of the decellularized TC. The short time of chondrogenic *in vitro* culture was selected on the basis that (1) immature cartilaginous tissues generated with hNCs are capable to develop into high-quality cartilage tissues *in vivo*,¹⁸ and (2) a rapid manufacturing protocol would be preferable for its implementation in clinics for the repair of tracheal wall defects in patients.²⁷

Revitalized LPTCs were implanted in subcutaneous pockets of nude mice to investigate the extent of matrix deposition by the hNCs in such an *in vivo* permissive environment. Histological examination of tissues retrieved 4 weeks after implantation demonstrated a large number of human (ALU-positive) cells within the pores of the samples, as well as a newly deposited GAG-positive matrix. These data indicated that hNCs survived well within the LPTCs and produced a cartilaginous matrix. However, it was observed that cells remained primarily confined

within the holes, probably due to their incapacity to migrate through the ring of the dense matrix lining the edges of the holes. The removal of this ring of matrix through an additional enzymatic digestion step of the LPTCs (“deGAG treatment”) as described by Nürnbergger et al.²⁴ could be considered to improve the matrix colonization by NCs.

A proof-of-principle study was also performed to assess the feasibility of using the NC-revitalized LPTCs for the repair of tracheal wall defects in rabbit. As a total tracheal replacement was not targeted with tissue-engineered grafts, it was decided to perform the interventions on the neck part of a rabbit trachea. Thus, a possible tissue resection size was limited up to 4 tracheal rings. However, in accordance with Remlinger et al.,²⁸ the hereby created 6×4 mm full-thickness defect can be considered an experimental representation of tracheal reconstruction.²⁸ Our results showed that the grafted tissues were functionally compatible and suitable for a partial tracheal replacement, holding a stable shape and supporting a tracheal lumen. Histological analyses demonstrated an abundant deposition of GAG around cell lacunas in explanted revitalized LPTCs, in contrast to non-revitalized LPTCs. However, no clear conclusion can be drawn on the origin of cells producing the new matrix *in vivo*. Further experiments with a cell-tracking system should be then performed to reveal the direct contribution of NCs in new cartilage formation at the implantation side.

The airway mucosal epithelization was observed on the inner surface of both revitalized and non-revitalized LPTC grafts in the orthotopic setting, suggesting that LPTCs can support epithelial ingrowth *in vivo*. However, relatively small cartilage grafts in our proof-of-principle rabbit study were used. For large segment reconstruction, mucosal growth over the LPTCs would take a considerable time, during which bacterial colonization of the graft could occur. Therefore, further investigations must be undertaken to develop an efficient *in vitro* epithelialization strategy of the NC-revitalized LPTCs, possibly using epithelial cells that can be harvested from the same tissue source of the NCs,²⁹ for a more streamlined clinical translation of this approach.

Conclusion

This study validates the feasibility of using LPTCs, revitalized by NCs, as grafts for the repair of tracheal wall defects. Future studies in larger animal models will be required to test the feasibility of the strategy for the treatment of long-segment tracheal stenosis.

Author Contributions

IM, AB, VP, HR and DL conceived and designed the study. DB performed experiments and generated data of the *in vitro* revitalization of LPTC tissues and *in vivo* ectopic and orthotopic

studies. AL and IK performed harvesting of the cadaver tracheal specimens, their decellularization, and shipment. JD conducted the quality control studies and helped with the culture of human chondrocytes. SN and HR performed the laser ablation of the TC tissues. SP performed the micro-CT analyses and the ectopic *in vivo* study. MH performed the histological quantifications and acquired the histological images. MK and OK conducted part of the culture of the grafts for the orthotopic study and helped with the editing of the manuscript. IK and AB performed the statistical evaluation. DB, AB, OK, IK, SN, and IM wrote the paper. All authors read and approved the final draft of the manuscript.

Acknowledgments and Funding

We thank our colleagues Dr. Diganta Kakaty and Lev Kim for their assistance in cell culture work. We are very grateful to Prof. Evgenia Kogan, Dr. Nickolay Zharkov, Prof. Natalia Serova, Dr. Olga Pavlova (Sechenov University), and Ms. Francine Wolf (University-Hospital Basel) for their assistance in the histological and immunohistochemical analyses. We are also thankful to Michael Baumgartl for the irradiation sterilization of initial tracheal tissue specimens. The author(s) disclosed receipt of the following financial support for the research, authorship and/or publication of this article: This work was supported by the Ministry of Education and Science of the Russian Federation (grant number 14.614.21.0001, ID RFMEFI61417X0001).




Declaration of Conflicting Interests

The author(s) declared no potential conflicts of interest with respect to the research, authorship, and/or publication of this article.

Ethical Approval

All procedures were conducted with the approval of the Basel Ethics Committee and Swiss Federal Veterinary Office. All human samples were collected with informed consent given by the involved individuals and/or relatives. All animals were treated in agreement with the Swiss legislation with approval by the Veterinary Office of Canton Basel-Stadt (permission # 1797, for experiments with mice) and the Local Ethic Committee of Sechenov University (permission # 07-05, for experiments in rabbits).

ORCID iDs

Ilya Klabukov  <https://orcid.org/0000-0002-2888-7999>
Ivan Martin  <https://orcid.org/0000-0001-6493-0432>
Andrea Barbero  <https://orcid.org/0000-0001-5252-789X>

References

- Chiang T, Pepper V, Best C, Onwuka E, Breuer CK. Clinical translation of tissue engineered trachea grafts. *Ann Otol Rhinol Laryngol*. 2016;125(11):873-85. doi:10.1177/0003489416656646.
- Law JX, Liao LL, Aminuddin BS, Ruszymah BHI. Tissue-engineered trachea: a review. *Int J Pediatr Otorhinolaryngol*. 2016;91:55-63. doi:10.1016/j.ijporl.2016.10.012.
- Damiano G, Palumbo VD, Fazzotta S, Curione F, Lo Monte G, Brucato VMB, et al. Current strategies for tracheal replacement: a review. *Life*. 2021;11(7):618. doi:10.3390/life11070618.
- Udelsman B, Mathisen DJ, Ott HC. A reassessment of tracheal substitutes—a systematic review. *Ann Cardiothorac Surg*. 2018;7(2):175-82. doi:10.21037/acs.2018.01.17.
- Guimarães CF, Gasperini L, Marques AP, Reis RL. The stiffness of living tissues and its implications for tissue engineering. *Nat Rev Mater*. 2020;5(5):351-70. doi:10.1038/s41578-019-0169-1.
- Xu Y, Li Y, Liu Y, Li H, Jia Z, Tang Y, et al. Surface modification of decellularized trachea matrix with collagen and laser micropore technique to promote cartilage regeneration. *Am J Transl Res*. 2019;11(9):5390-403.
- Giraldo-Gomez DM, García-López SJ, Tamay-de-Dios L, Sánchez-Sánchez R, Villalba-Caloca J, Sotres-Vega A, et al. Fast cyclical-decellularized trachea as a natural 3D scaffold for organ engineering. *Mater Sci Eng C Mater Biol Appl*. 2019;105:110142. doi:10.1016/j.msec.2019.110142.
- Zang M, Zhang Q, Chang EI, Mathur AB, Yu P. Decellularized tracheal matrix scaffold for tissue engineering. *Plast Reconstr Surg*. 2012;130(3):532-40. doi:10.1097/PRS.0b013e31825dc084.
- Hussey GS, Nascari DG, Saldin LT, Kolich B, Lee YC, Crum RJ, et al. Ultrasonic cavitation to prepare ECM hydrogels. *Acta Biomater*. 2020;108:77-86. doi:10.1016/j.actbio.2020.03.036.
- Zhang Y, Xu Y, Liu Y, Dan Li, Yin Z, Huo Y, et al. Porous decellularized trachea scaffold prepared by a laser micropore technique. *J Mech Behav Biomed Mater*. 2019;90:96-103. doi:10.1016/j.jmbbm.2018.10.006.
- Liu Y, Nakamura T, Sekine T, Matsumoto K, Ueda H, Yoshitani M, et al. New type of tracheal bioartificial organ treated with detergent: maintaining cartilage viability is necessary for successful immunosuppressant free allotransplantation. *ASAIO J*. 2002;48(1):21-5.
- Zieber L, Or S, Ruvinov E, Cohen S. Microfabrication of channel arrays promotes vessel-like network formation in cardiac cell construct and vascularization *in vivo*. *Biofabrication*. 2014;6(2):024102. doi:10.1088/1758-5082/6/2/024102.
- Rotter N, Bonassar LJ, Tobias G, Lebl M, Roy AK, Vacanti CA. Age dependence of biochemical and biomechanical properties of tissue-engineered human septal cartilage. *Biomaterials*. 2002;23(15):3087-94. doi:10.1016/S0142-9612(02)00031-5.
- Kafienah WE, Jakob M, Démarteau O, Frazer A, Barker MD, Martin I, et al. Three-dimensional tissue engineering of hyaline cartilage: comparison of adult nasal and articular chondrocytes. *Tissue Eng*. 2002;8(5):817-26. doi:10.1089/10763270260424178.
- Pelttari K, Pippenger B, Mumme M, Feliciano S, Scotti C, Mainil-Varlet P, et al. Adult human neural crest-derived cells for articular cartilage repair. *Sci Transl Med*. 2014;6(251):251ra119. doi:10.1126/scitranslmed.3009688.
- Gay MHP, Mehrkens A, Rittmann M, Haug M, Barbero A, Martin I, et al. Nose to back: compatibility of nasal chondrocytes with environmental conditions mimicking a degenerated intervertebral disc. *Eur Cell Mater*. 2019;37:214-32. doi:10.22203/eCM.v037a13.

17. Fulco I, Miot S, Haug MD, Barbero A, Wixmerten A, Feliciano S, *et al.* Engineered autologous cartilage tissue for nasal reconstruction after tumour resection: an observational first-in-human trial. *Lancet*. 2014;384(9940):337-46. doi:10.1016/S0140-6736(14)60544-4.
18. Mumme M, Barbero A, Miot S, Wixmerten A, Feliciano S, Wolf F, *et al.* Nasal chondrocyte-based engineered autologous cartilage tissue for repair of articular cartilage defects: an observational first-in-human trial. *Lancet*. 2016;388(10055):1985-94. doi:10.1016/S0140-6736(16)31658-0.
19. Roth SP, Glauche SM, Plenge A, Erbe I, Heller S, Burk J. Automated freeze-thaw cycles for decellularization of tendon tissue—a pilot study. *BMC Biotechnol*. 2017;17(1):13. doi:10.1186/s12896-017-0329-6.
20. Power LJ, Fasolato C, Barbero A, Wendt DJ, Wixmerten A, Martin I, *et al.* Sensing tissue engineered cartilage quality with Raman spectroscopy and statistical learning for the development of advanced characterization assays. *Biosens Bioelectron*. 2020;166:112467. doi:10.1016/j.bios.2020.112467.
21. Chen W, Li C, Peng M, Xie B, Zhang L, Tang X. Autologous nasal chondrocytes delivered by injectable hydrogel for in vivo articular cartilage regeneration. *Cell Tissue Bank*. 2018;19(1):35-46. doi:10.1007/s10561-017-9649-y.
22. Grogan SP, Barbero A, Winkelmann V, Rieser F, Fitzsimmons JS, O'Driscoll S, *et al.* Visual histological grading system for the evaluation of in vitro-generated neocartilage. *Tissue Eng*. 2006;12(8):2141-9. doi:10.1089/ten.2006.12.2141.
23. Crowe AR, Yue W. Semi-quantitative determination of protein expression using immunohistochemistry staining and analysis: an integrated protocol. *Bio Protoc*. 2019;9(24):e3465. doi:10.21769/BioProtoc.3465.
24. Nürnberger S, Schneider C, Keibl C, Schädl B, Heimel P, Monforte X, *et al.* Repopulation of decellularised articular cartilage by laser-based matrix engraving. *EBioMedicine*. 2021;64:103196. doi:10.1016/j.ebiom.2020.103196.
25. Xu Y, Li D, Yin Z, He A, Lin M, Jiang G, *et al.* Tissue-engineered trachea regeneration using decellularized trachea matrix treated with laser micropore technique. *Acta Biomater*. 2017;58:113-21. doi:10.1016/j.actbio.2017.05.010.
26. Li Y, Xu Y, Liu Y, Wang Z, Chen W, Duan L, *et al.* Decellularized cartilage matrix scaffolds with laser-machined micropores for cartilage regeneration and articular cartilage repair. *Mater Sci Eng C Mater Biol Appl*. 2019;105:110139. doi:10.1016/j.msec.2019.110139.
27. Ott LM, Weatherly RA, Detamore MS. Overview of tracheal tissue engineering: clinical need drives the laboratory approach. *Ann Biomed Eng*. 2011;39(8):2091-113. doi:10.1007/s10439-011-0318-1.
28. Remlinger NT, Czajka CA, Juhas ME, Vorp DA, Stolz DB, Badylak SF, *et al.* Hydrated xenogeneic decellularized tracheal matrix as a scaffold for tracheal reconstruction. *Biomaterials*. 2010;31(13):3520-6. doi:10.1016/j.biomaterials.2010.01.067.
29. Pfenninger C, Leinhase I, Endres M, Rotter N, Loch A, Ringe J, *et al.* Tracheal remodeling: comparison of different composite cultures consisting of human respiratory epithelial cells and human chondrocytes. *In Vitro Cell Dev Biol Anim*. 2007;43(1):28-36. doi:10.1007/s11626-006-9000-6.